Ore Geology Reviews 81 (2017) 1236–1248

Contents lists available at ScienceDirect

Ore Geology Reviews

journal homepage: www.elsevier.com/locate/oregeorev

An overview of the platinum-group element nanoparticles in mantle-hosted chromite deposits

José M. González-Jiménez *, Martin Reich

Department of Geology and Andean Geothermal Center of Excellence (CEGA), FCFM, Universidad de Chile, Plaza Ercilla #803, Santiago, Chile.

ARTICLE INFO

Article history:
Received 12 April 2016
Received in revised form 14 June 2016
Accepted 22 June 2016
Available online 23 June 2016

Keywords:
Platinum-group elements
Mineral nanoparticles
Nanominerals
Chromite deposits
Nanogeoscience

ABSTRACT

This paper reviews the occurrence of platinum-group elements nanoparticles (PGE-NPs) in mantle-hosted chromite deposits, showing that PGE-NPs are more frequently found in these deposits than previously thought. A comparison of published experimental data with observations in natural samples reveal that PGE-NPs might form at the pressure (1–0.5 GPa), temperature (~1200 °C) and fO_2 (FMQ ± 1) conditions in which chromite deposits form in the upper mantle. The crystallization of PGE-NPs may take place earlier or simultaneously to the segregation of chromite and/or sulfide liquids from silicate melts. If the PGEs are dissolved in the silicate melt, the segregation of PGE-NPs could be linked to local changes in fO_2 and fS_2 during the early crystallization of chromite and/or olivine. Mobile crystals of chromite and droplets of sulfide melts entrained in the basaltic parent melt may also play an additional role as physical collectors of PGE-NPs, providing a complementary or even an alternative mechanism for the fractionation of PGEs in high temperature silicate melts. Furthermore, hydrothermal alteration of the chromite deposits during seafloor metamorphism or exhumation (i.e., retrograde metamorphism) of upper mantle rocks has also a significant effect on the internal structure of the oxides and sulfides that host the PGE-NPs. Frequently, PGE-NPs are found along the replacement contacts between primary and secondary minerals, suggesting that PGE-NPs can also form during low temperature alteration events (200–600 °C). Finally, heating events overimposed on chromite deposits previously affected by hydrous metamorphism may enhance fluid infiltration subsequently triggering chemical, mineralogical, or textural responses in the oxide or sulfide matrices hosting the PGE-NPs, promoting coarsening of metal nanoparticles. The interplay between these processes can explain the wide spectrum of particle sizes of PGE inclusions that are observed in many altered chromite deposits, which can vary from a few nanometers to larger than a micron. These studies provide evidence that PGE-NPs can eventually form under a wide spectrum of thermal (and pressure) conditions, and show that aqueous fluids may play a relevant role in producing PGE-NPs during metamorphism and metasomatism of mantle-hosted chromite deposits.

Contents

* Corresponding author: Departament of Geology, Universidad de Chile, Plaza Ercilla #803, Santiago, Chile
E-mail address: jmgonzj@ing.uchile.cl (J.M. González-Jiménez).

http://dx.doi.org/10.1016/j.oregeorev.2016.06.022
0169-1368/

1. Introduction

In nature, minerals can occur as nanofilms, nanorods or nanoparticles when having one, two or three dimensions reduced to the nanoscale, respectively. They can occur as mineral *nanoparticles* when they also exist in larger (micrometer-scale) sizes, and as *nanominerals* when they only exist within this size range (Fig. 1). When occurring in minerals, nanoparticles can now be sampled into thin foils for imaging and characterization under the transmission electron microscope (TEM) by means of focussed ion beam-field emission scanning electron microscopy techniques (FIB-FE-SEM) (Wirth, 2004, 2009; Lee, 2010; Ciobanu et al., 2011). These high-resolution analytical methods are providing an unprecedent view of metal incorporation in ore minerals since examination of the textures, composition and structures of metal nanoparticles and their host matrices can be now obtained at any location on a mineral grain (Ciobanu et al., 2011). This new information helps us to unravel what is the relationship between mineral particle size and physico-chemical properties, a critical issue when defining the potential impact of nanogeoscience in mineral research (Hochella, 2008).

Since last decade, an increasing amount of studies are showing that minerals, apart from influencing or driving most physical, chemical and biological processes on Earth, also exert their influence through particle size. In particular, minerals can behave very differently at the nanoscale comparing with their bulk counterparts. Studies have documented significant variations in structural, thermodynamic and catalytic properties when one or more dimensions of minerals are reduced to the nanoscale, i.e., below one micron, although novel material properties commonly arise between 1 and 100 nm. These variations are most likely due to differences in surface and near-surface crystal structure, as well as shape and large surface area relative to size (Banfield and Navrotsky, 2001; Navrotsky et al., 2008; Reich et al., 2011). There have been excellent reviews of some of these issues, and the readers are referred to Hochella (2002), Hochella (2008) and Lee Penn (2012).

In the field of ore deposits research and in economic geology in general, mineral nanoparticles and nanominerals of economic metals are only recently beginning to receive attention they deserve (Reich et al., 2011). Most of the studies have focused on gold, and into a lesser extent the other noble metals, in refractory sulfide phases and in supergene profiles (e.g., Saunders, 1990; Palenik et al., 2004; Reich et al., 2005, 2006, 2010; Ciobanu et al., 2009, 2012; Hough et al., 2008; Reith et al., 2010, 2012, 2016; Zhmodik et al., 2012; Reich and Vasconcelos, 2015), and results strongly suggest that nanoscale processes are key factors

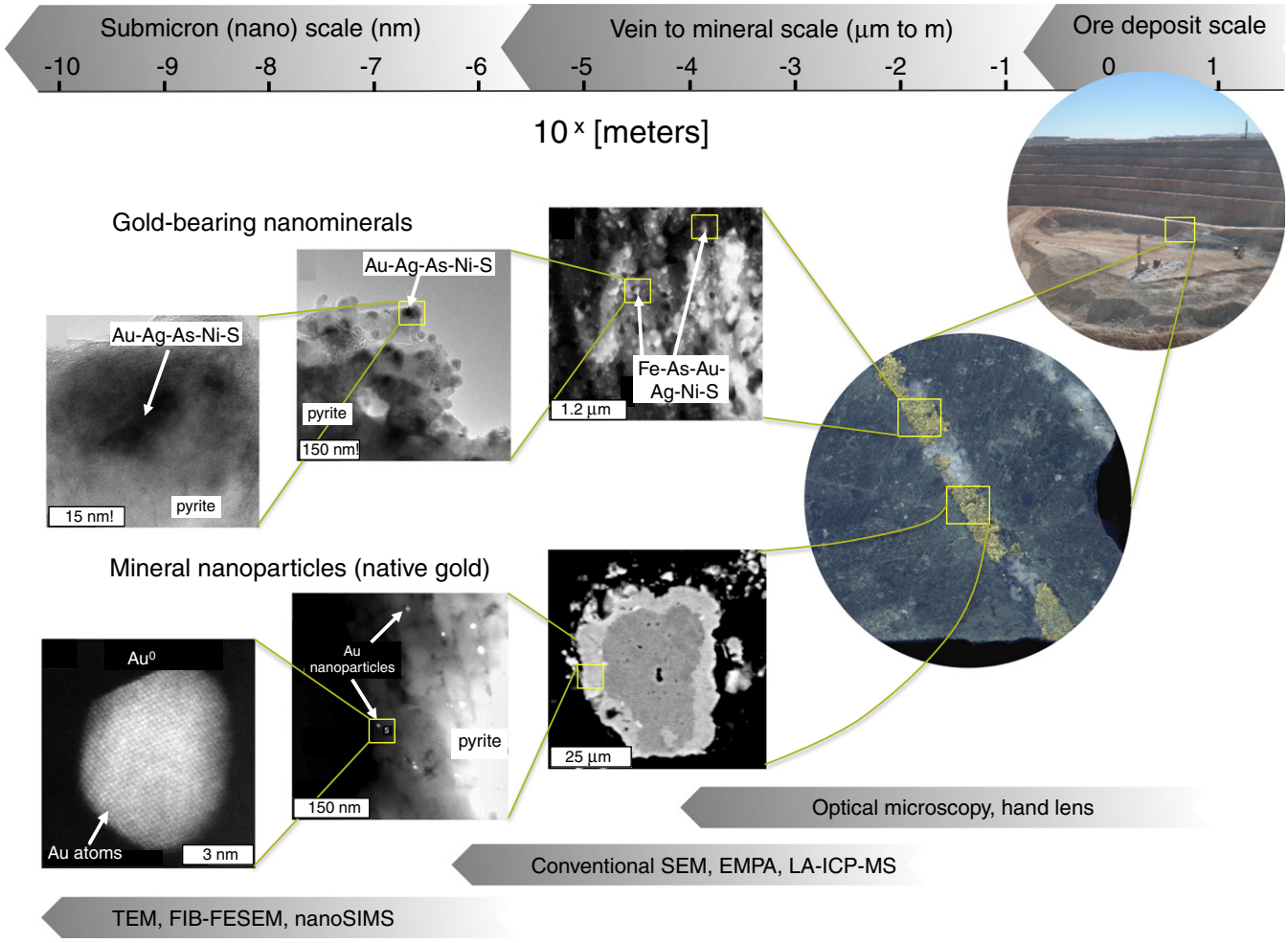

Fig. 1. The dimensional scale of the earth sciences and mineral deposits research. Horizontal scale on top is depicted in $10^{\times}$ meters, shows ~10 orders of magnitude difference in scale between an ore body (upper right) and metal nanoparticles (left) contained in vein-hosted pyrite grains (center picture, right side). TEM images are taken from Reich et al. (2005, 2006) and Deditius et al. (2011). Imaging techniques suitable for each dimensional range are for are shown at the bottom (see text for acronyms).

that may control large-scale ore deposition in hydrothermal settings and near-surface environments (e.g., Hannington et al., 2016).

In this context, the potential role of nanoscale phases during the selective partitioning of the others noble metals of the platinum group (i.e., platinum-group elements, PGEs: Os, Ir, Ru, Rh, Pt and Pd) has been little explored, particularly under the high-temperature typical of magmatic processes. The PGEs are much less abundant than gold and silver in the Earth's crust, and they are almost exclusively found in ores associated with mafic and ultramafic rocks. In these ores the PGEs occur at the trace to ultra-trace levels (ppm to ppb) and their budget in terms of host minerals is still discussed (e.g., O'Driscoll and González-Jiménez, 2016 and references therein). Most of these PGE-bearing ores are formed as a result of high-temperature magmatic processes, where the highly siderophile and chalcophile PGEs are segregated from mafic or ultramafic magmas into metal-rich immiscible melts (i.e., oxide, sulfide, arsenide, telluride, and bismuthide). In particular, PGEs have been documented in chromite ± magnetite ± sulfide ± arsenide ores associated with komatiites, layered or concentrically zoned mafic-ultramafic complexes within or at the boundaries of cratons as well as in the mantle or mantle-crust section of ophiolite complexes (Gervilla and Leblanc, 1990; Leblanc et al., 1990; Ballhaus et al., 2001; Cabri, 2002; Arndt et al., 2006; Hanley, 2007; Prichard et al., 2013; Piña et al., 2015; Holwell et al., 2015; Barnes and Ripley, 2016).

Due to their importance as PGEs reservoirs and the complex postmagmatic histories that usually affect them, the emphasis of this review is placed on chromite deposits associated to the mantle section of ophiolite complexes, although PGE ores from the layered mafic-ultramafic continental intrusion of the Bushveld Complex (South Africa) are also briefly discussed because they represent the first known examples of magmatic ores hosting PGE-NPs. Platinum deposits in Alaksan-Aldan-Ural-type complexes will be not covered here because PGE-NPs have not been reported in these ores yet. The aim of this paper is by no means intended to present a deep literature review of magmatic ore deposits and their genesis, but rather to provide a first view of noble metal nanoparticle in the mafic-ultramafic ore systems, an aspect of nanogeoscience that has been little explored. The underlying scheme of this study is not just devoted to describe nanoparticles as isolated entities in their carrier phases; rather, we aim to outline how the study of PGE-NPs can actually provide new insights about local and large-scale processes governing precious metal concentration in chromite-rich ores.

Three examples were chosen on the basis of our interest in linking chemical heterogeneity with the occurrence of nano- and micron-sized mineral inclusions in the suite of minerals that usually host PGEs in the ore deposits (i.e., oxides and base-metal sulfides). We discuss the formation of PGE-NPs at magmatic conditions in the upper mantle where the chromite deposits occur, and their potential modification under different thermal regimes and fluid/rock ratios during crustal emplacement. Thus we report PGE-NPs bearing chromite deposits affected by: (1) low-temperature serpentinization in an ocean-floor setting (Caridad chromite deposit in the Eastern Cuban ophiolites), (2) retrograde eclogite to greenchist metamorphism (chromite deposits of the Dobromirtsi massif, southern Bulgaria), and (3) prograde metamorphism associated with granite intrusions (Loma Baya chromite deposit of southwestern Mexico). Through these examples we emphasize the importance and potential utility of mineral nanoparticles in understanding the magmatic and post-magmatic evolution of the PGE-bearing ores, and also explore their potential role as agents for noble metal transport/concentrations in ore systems.

2. Previous reports of PGE-NPs in high-temperature experiments and magmatic chromite deposits in the crust

2.1. PGE-NPs sythethised in experiments under magmatic conditions

The notion that PGE-NPs could form in basaltic melts at high temperatures (>1000 °C) might be supported by a series of experiments in the last decade (Bockrath et al., 2004; Ballhaus et al., 2006; Finnigan et al., 2008; Helmy et al., 2013). However, the economic geology community has overlooked this evidence so far. In the next paragraphs we provide a brief overview of the main results of these studies.

The pioneering experiment study by Bockrath et al. (2004) involved a basaltic melt with a picrite composition, which was doped with up to 5 wt% Cr_2O_3 and 1 wt% RuO_2. To promote crystal growth, the mix was fused at 1360 °C for 5 h, and then cooled slowly at rate of 10°/h up to 1200 °C, kept there for another 5 h, and then quenched. The experiment was undertaken in a graphite capsule within a piston cylinder press. At 0.5 GPa the charge crystallized olivine, skeletal clinopyroxene, euhderal chromite, and spherical Fe-free Ru metal nugget (Fig. 2a). According to Bockrath et al. (2004) most of the Ru nuggets were smaller than 1 μm (Fig. 2b) and nucleated on chromite surfaces, whereas only a few larger nuggets were found suspended in the glass.

Finnigan et al. (2008) also produced PGE-NPs (Ir-Pt alloys and Ru-S) in the course of experiments involving crystallization of chromite from a silicate melt (Fig. 2c-d). The latter experiments were peformed by calcination of finely powdered natural alkali olivine basalt to which powdered natural chromite and spinel crystals were added. In these experiments, Ir-Pt nanoparticles were formed between 1370 and 1400 °C in sulfur-free environment, whereas nanoparticles of Ru-S nanoparticles were crystallized at much lower temperature (1200 °C) but in silicate melts containing sulfur.

Helmy et al. (2013) doped Fe-S and Fe-Cu-S melts with traces of Pt and As and equilibrate these compositions between 950 and 1180 °C. Using high-resolution TEM they were able to find a wide range of Pt-As nano-associations, including poorly ordered (Pt, As) *n* clusters, crystalline $PtAs_2$ nanoparticle platelets and nanometer-sized droplets of Pt-enriched melts (Fig. 2e-f). Based on these results, Helmy and co-workers suggested that at high temperatures (>1000 °C) Pt and As self-organize to form nanoparticles in silicate melts, well before the melt has reached Pt and As concentrations at which discrete Pt arsenide minerals become stable phases (Fig. 2e-f).

The results provided in all these previous experiments predict that PGE-NPs are stable at high temperatures in magmatic systems although the mechanism(s) of formation and preservation of these particles during cooling or post-magmatic alteration remains unclear and further experimental studies are needed.

2.2. Previous reports of PGE-NPs in crustal-hosted magmatic PGE deposits

In one of the few studies available, Wirth et al. (2013) documented the occurrence of PGE-NPs in base-metal sulfides (BMS) from PGE-rich chromitite and melanorite pegmatites from the Merensky Reef. This is one of the three deposits exploited for PGEs in the Bushveld Complex in South Africa (Campbell et al., 1983; Tredoux et al., 1995; Vermaak, 1995; Ballhaus and Sylvester, 2000; Prichard et al., 2004; Naldrett, 2004; Godel et al., 2007; Mungall and Naldrett, 2008; Scoates and Fiedman, 2008; Rose et al., 2011). Wirth et al. (2013) presented TEM observations on thinned BMS grain foils that were previously selected and retrieved using FIB-FESEM to avoid large PGM inclusions. They identified crystals of <50 nm of Ru-Rh-Pt arsenides hosted in pyrrhotite ($Fe_{1-x}S$) and pyrite (FeS_2), Ru-Rh-Os, Ru-Rh-Pt-Ir, and Ru-Rh-Pt sulfides included in pyrrhotite and pentlandite $(Fe,Ni)_9S_8$, and one ~250 nm nanocrystal of Pt-Au-Hg within chalcopyrite ($CuFeS_2$) (Fig. 3a-d). According to these authors, PGE-NPs found in pyrrhotite were heterogeneously distributed and differently oriented with respect to the host polycrystalline sulfide matrix. In contrast, the PGE-NPs found along interfaces between pyrrhotite and pyrite (i.e., Ru-Rh-bearing arsenides) or between pyrrhotite and pentlandite (i.e., Ru-Rh-bearing sulfides) were arranged like "pearls on a string", parallel to the grain boundary. Wirth et al. (2013) also observed that Ru-Rh arsenides can occur in solid solution in pyrite, and that the Ru-sulfide crystals may display identical orientation relationship with the pentlandite host.

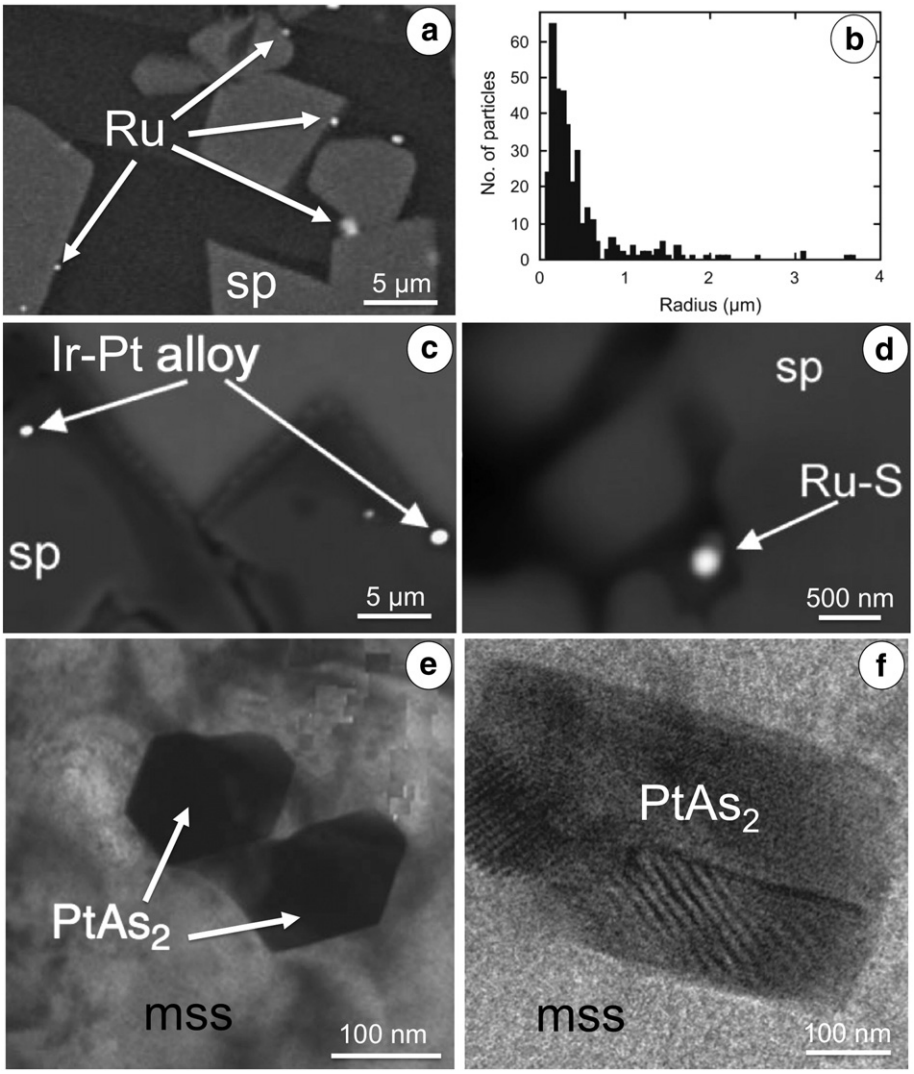

Fig. 2. Backscattered electron images of PGE-NPs syntethized in high-temperature experiments. (a) Ru^0 nanoparticles nucleated on chromite surfaces crystallized at from a silicate melt with a picritic composition. This experiment was performed by Bockrath et al. (2004) at 1360–1200 °C, doping the silicate melt with 5 wt% Cr_2O_3 and 1 wt% RuO_2. (b) Size distribution of 361 Ru metal nuggets in the experimental charge illustrated in (a). The median diameter is 0.29 μm. All Ru metal nuggets smaller than ~700 nm in diameter are attached to chromite grains, whereas metal nuggets larger than 1 μm generally occur suspended freely in the silicate glass. (c–d) Ir-Pt crystallized between 1400 and 1370 °C in a sulfur-free environment. (d) Nanoparticles of Ru-S were crystallized at much lower temperature (1200 °C) but in silicate melts containing sulfur. Experiments illustrated in (c) and (d) were carried out by Finnigan et al. (2008). (e–f) Nanoparticles of Pt-arsenides in monosulfide solid solution (*mss*), indicating the possible crystallization of PGE-NPs before the segregation of immisicible sulfide liquids from basaltic melts at temperatures above 1000 °C (Helmy et al., 2013). Abreviations: Ru: native ruthenium, Sp: spinel, Mss: monosulfide solid solution, Ir-Pt: iridium-platinum alloy, Ru-S: ruthenium sulfide.

In a more recent study, Junge et al. (2015) also used FIB-FESEM techniques coupled with TEM observations to study pentlandite grains with elevated concentrations of PGEs from the Platreef at Mogalakwena Mine (Sandsloot pit) in the northern Bushveld Complex, and from the UG-2 chromitite at the Karee Mine. The cited authors detected the presence of a variety of PGE-NPs within the pentlandite, including Pt-Pd-Sn nano-phases, Pt-bismuthides and Pt-tellurides (Platreef only), a Pd-Sn nanophase (most likely atokite [Pd_3Sn]; UG-2 only) and Pt-(Fe, Cu) alloys (in both localities). The reported PGE-NPs are idiomorphic with sizes smaller than 100 nm (Fig. 3e-f); they are heterogeneously distributed in the matrix, and no crystallographic match was observed with respect to the host pentlandite structure. Furthermore, Junge et al. (2015) identified PGE-rich domains substituting for Ni and/or Fe in the crystal structure of the UG-2 chromitite. These consist of small (10 to 100 nm) specks or orientated lamellar nano-structures with high concentrations of Rh and Ir that show a coupled depletion in Ni and Fe, as detected by TEM-EDS. Also, the authors observed that a large proportion of Pd, even at elevated concentrations, is homogenously distributed and most likely contained in solid solution in pentlandite.

The studies by Wirth et al. (2013) and Junge et al. (2015) indicate that the idiomorphic, heterogeneously distributed PGE-NPs do not show any structural match with that of the host BMS. These results suggest that PGE-NPs could form earlier than the BMS, ruling out an origin by low-temperature exsolution. In the model proposed by Wirth et al. (2013) and Junge et al. (2015), noble metal micro-inclusions or "nuggets" (Tredoux et al., 1995) composed of PGEs plus sulfur and/or metalloids (As or Sn) may form early in the high-temperature silicate melt, acting as nuclei for the adhesion of sulfide liquid droplets once the melt reached sulfide saturation. Assuming that PGEs are dissolved in the silicate melt as binary PGE-O and/or PGE-S complexes, Wirth et al. (2013) proposed that clusters of hundreds of atoms of metallic PGEs or PGEs + metalloids must have been segregated at the initial stage of the cooling process, thus overcoming the problem of crystal nucleation under low, undersaturated concentrations of PGEs. The segregation of these atomic clusters may have been promoted by changes in the activity of silica ($a SiO_2$) and/or in the oxygen fugacity (fO_2), as soon as minerals such as chromite and/or olivine started to crystallize early from the melt (e.g., Ballhaus and Sylvester, 2000; Mungall, 2005; Wirth et al.,

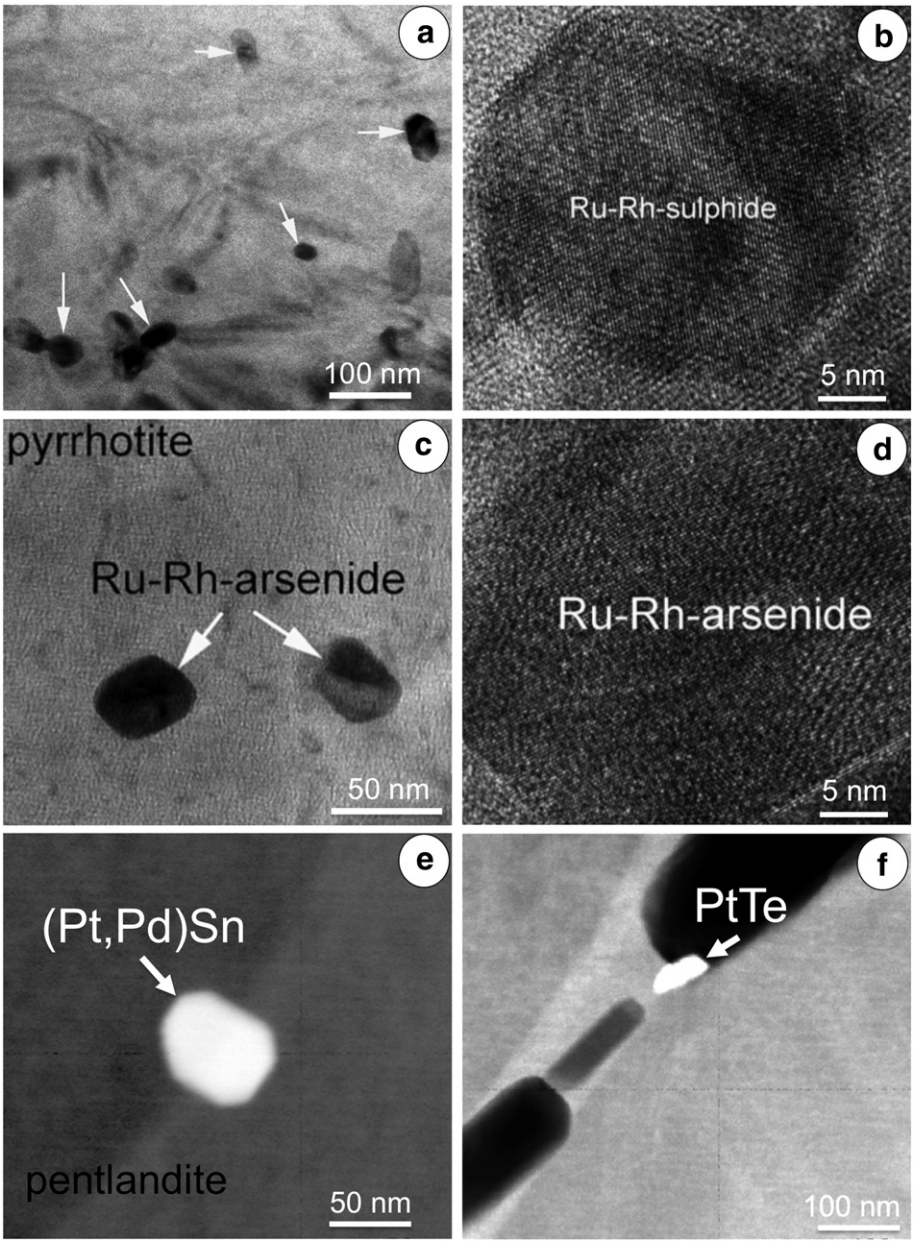

Fig. 3. Backscattered electron images of PGE-NPs included in base-metal sulfides from the Bushveld Complex. (a–d) are images from Wirth et al. (2013) whereas (e) and (f) are images from Junge et al. (2015).

2013). These atomic PGE clusters may have coalesced in the silicate *milieu* to form larger PGE-NPs (Tredoux et al., 1995). Upon further cooling, sulfur saturation was achieved in the silicate melt, causing the formation of droplets of an immiscible monosulfide liquid. Within this scenario, the exsolving sulfide melts may physically entrain or capture the PGE-NPs producing PGE-rich sulfide melts (Laurenz et al., 2013).

The model proposed by Wirth et al. (2013); Laurenz et al. (2013) and Junge et al. (2015) challenges the classic model where a sulfide liquid primarily collects PGEs solely as dissolved cations in the magma owing their relatively high sulfide/silicate partition coefficient (e.g., Campbell et al., 1983; Peach et al., 1990; Roy-Barman et al., 1998; Mungall and Naldrett, 2008; Fonseca et al., 2011; Laurenz et al., 2013; Patten et al., 2013; Pruseth and Palme, 2004; Mungall and Brenan, 2014). Rather, as stated by Helmy et al. (2013) '*… if all highly siderophile elements associate to nanophases in undersaturated melts, the distribution of the noble metals between silicate, sulfide, and metal melts will be controlled by the surface properties of nano-associations, more so than by the chemical properties of the elements…*'. Thus, it is likely that a monosulfide liquid segregated at high temperature can trap PGE metal clusters and/or precursors of PGE-NPs as suggested by Tredoux and co-workers two decades ago. After their physical entrainment many PGE-NPs would dissolve into the sulfide liquid, while under further cooling the solidified *mss* might still exsolve discrete PGMs (Wirth et al., 2013). This can explain the observation of Ru-Rh arsenides and Ru-sulfide nanocrystals forming lamellar arrays along interfaces between pyrrhotite and pyrite or between pyrrhotite and pentlandite from the Merensky Reef (Wirth et al., 2013), and lamellar nanostructures with high concentrations of Rh and Ir substituting Ni and/or Fe in the crystal structure of pentlandite of the UG-2 chromitite (Junge et al., 2015). These observations suggest that under the absence of bonding partners (e.g., As, Sn, Bi, Te) necessary for the formation of PGE-NPs at high temperature, some PGEs will remain locked in the crystal structure of pentlandite. These structurally bound PGEs may be exsolved upon cooling as nano- to micron-sized PGE particles (Junge et al., 2015), similarly to those in natural samples and experimental runs (Mackovicky et al., 1986; Ballhaus and Ulmer, 1995; Peregoedova and Ohnenstetter, 2002).

3. PGE-NPs in mantle-hosted chromite deposits

3.1. Ir-Pt mineral nanoparticles in base-metal sulfides of the Caridad chromite deposit (Eastern Cuba): effects of seafloor metamorphism

The Caridad chromite deposit is one of the ten Cr-rich chromite ore bodies being mined for Cr in the small mining district of Sagua de Tánamo in Cuba (González-Jiménez et al., 2011). It is a small body of up to ~100,000 tonnes of massively textured chromite ore, which lies almost in the centre of the Mayarí-Baracoa Ophiolitic Belt (MBOB) in eastern Cuba (Murashko and Lavandero, 1989; Proenza et al., 1999; Gervilla et al., 2005). Mineralogical data coupled with studies of stable isotopes of hydrogen, oxygen and carbon suggest that this chromite deposit and their hosting mantle dunites were partly altered during ocean-floor metamorphism (Proenza et al., 2003). The alteration sequence includes a first event of serpentinization, followed by a hydrothermal alteration event that produced chloritization and formed thin veins of calcite. The Caridad chromite deposit contains abundant inclusions of micrometer-sized PGMs (laurite (RuS_2), irarsite (IrAsS), cuproiridsite ($CuIr_2S_4$)) coexisting with BMS (millerite (NiS), heazlewoodite (Ni_2S_3), pentlandite and minor chalcopyrite) that have elevated concentrations of PGEs (up to 8.9 wt% Ru, 3.6 wt% Os, 0.41 wt% Ir, and Pt and Pd invariably below 1 wt%; González-Jiménez et al., 2012). These PGMs and BMS are located in both unaltered (i.e., cores of chromite) and altered zones of the chromitite (i.e., open fractures cutting the chromite grains and the interstitial serpentinized matrix between the chromite grains).

A detailed re-examination of these PGE-bearing Ni-Fe-Cu sulfides reported by González-Jiménez et al. (2012) using FESEM has now allowed the identification of discrete micro- to nano-scale inclusions of Ir-Pt alloys within these sulfides. Micrometer-sized inclusions of Ir-Pt alloys are associated with chalcopyrite and pentlandite grains found in both unaltered and altered zones of the chromitite (Fig. 4a-b). In contrast, nanocrystals of Ir-Pt alloys occur exclusively in the interface between pentlandite and heazlewoodite in altered zones of the chromitites. These PGE-NPs or "nanoalloys" form clusters around larger, micrometer-sized Ir-Pt alloys hosted in the BMS (Fig. 4c), or more commonly single sphere-like nanograins (<250 nm) aligned along the interface (i.e., replacement front) between partly desulfurized pentlandite and secondary heazlewoodite (Fig. 4d).

The fact that the BMS grains containing PGE-NPs (Ir-Pt alloys) are found in all textural zones of the chromitite (i.e., unaltered and altered; Fig. 4a-b) supports a common magmatic origin. Even though the micrometer-sized Ir-Pt alloys may have been formed at low temperatures (<600 °C) via exsolution of the PGEs that were initially dissolved within the structure of the *mss* at much higher temperatures (Mackovicky et al., 1986, 1988; Ballhaus and Ulmer, 1995; Peregoedova and Ohnenstetter, 2002), the experimental results of Peregoedova et al. (2004) indicate that these PGE alloys may have also been released from the *mss* at magmatic temperatures (~1000 °C). Under both scenarios, Ir-Pt alloys may form either by segregation of these metals in solid solution within the *mss* and/or through coalescence of Ir-Pt nanoalloys. PGE-NPs nanoparticles may have crystallized directly from the silicate melt *before* (*or coeval*) the segregation of the sulfide liquid from which the sulfide host crystallized, similarly as documented in the experiments by Helmy et al. (2013) for nanoparticles of PtAs.

As noted above, the Ir-Pt nanocrystals (~700 nm in diameter) synthesized in experiments have been observed to crystallize directly from basaltic melts at the P-T-fO_2 conditions relevant for the formation of chromite deposits in the upper mantle, i.e., P ~ 0.5 GPa, T ~ 1300–1400 °C and fO_2 ~FMQ (see Figure 4a in Finnigan et al., 2008). According to the experimental results by Finnigan et al. (2008), the crystallization of these PGE-NPs is likely controlled by fO_2 gradients in the proximities of growing chromite crystals. In their model, these authors assumed that sulfur-poor melts contain PGE speciated as oxygen-bearing PGE complexes. Finnigan et al. (2008) demonstrated that even if the melt is undersaturated with respect to the PGEs, a small decrease in fO_2 of the melt – resulting from chromite precipitation from or re-equilibration with the basaltic melt –may trigger PGEs nucleation in the form of metal alloys on the margins of larger chromite grains. In this model, the PGEs should fractionate between each another because they have different oxidation states in the melt. In basaltic silicate melts, Ru dissolves either as tetravalent or trivalent, Os and Ir

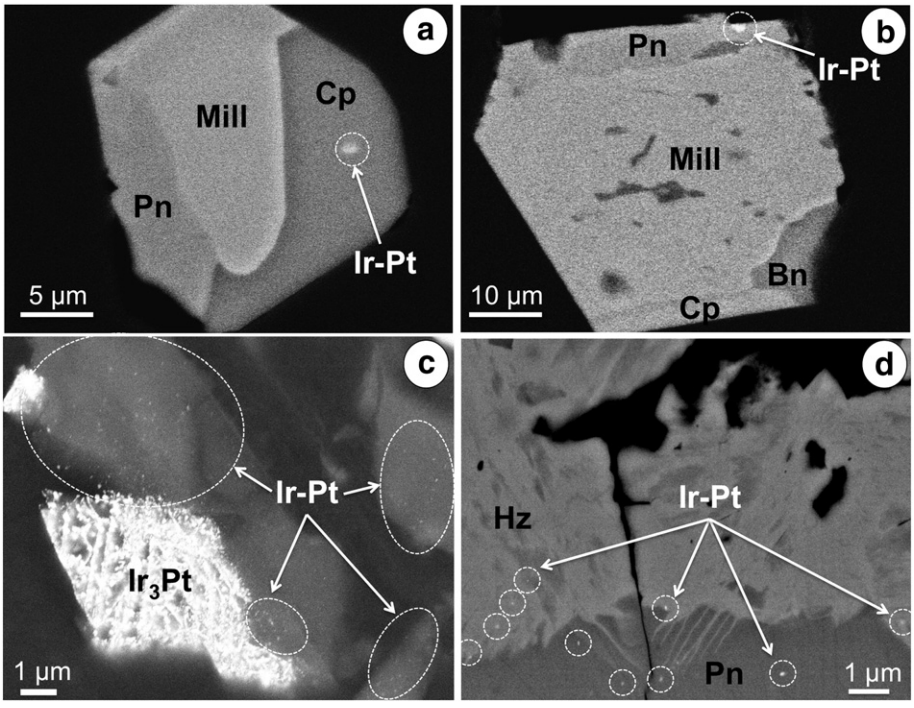

Fig. 4. Backscattered electron images obtained using FESEM of PGE-NPs included in base-metal sulfides hosted in the Caridad chromite deposit (eastern Cuba) Abbreviations: Pn: pentlandite, Mill: millerite, Hz: heazlewoodite, Cp: chalcopyrite, Bn: bornite, Ir-Pt: iridium-platinum alloy.

predominantly trivalent, whereas Ir Rh and Pt are divalent and Pd is monovalent (Borisov et al., 1994; Borisov and Palme, 1995, 1997, 2000; O'Neill et al., 1995; Ertel et al., 1999; Borisov and Nachtweyh, 1998; Borisov and Walker, 2000; Fortenfant et al., 2006; Fonseca et al., 2011, 2012; Laurenz et al., 2013). These observations are consistent with the fact that abundant crystals of Os-Ir-Ru minerals (i.e., laurite-erlichmanite and irarsite) are hosted within chromite grains of the Caridad deposit (González-Jiménez et al., 2012). Similarly but from an experimental viewpoint, Matveev and Ballhaus (2002); Bockrath et al. (2004) and Ballhaus et al. (2006) have reported the nucleation of abundant particles of Ru, Os and Ir metal on chromite surfaces, but much larger-sized metallic alloys of Pt and Pd in the silicate glass. Notwithstanding, the particles of Pt-bearing alloys produced in the experiments of Matveev and Ballhaus (2002) and Bockrath et al. (2004), are larger (>1 μm) than Ir-Pt occurring nanoparticles in the Caridad chromites and in the experimental runs by Finnigan et al. (2008). This size difference may be related to physico-chemical factors other than changes in fO_2 – for example, thermodynamic and kinetic controls at the nanoscale, including temperature and size dependent coarsening effects such as Ostwald ripening (Reich et al., 2006). Alternatively, the observed Ir-Pt nanoparticles in Caridad could correspond to oxygen or sulfur-bearing Ir-Pt nanometric compounds that may have been entrained as immiscible droplets by the immiscible sulfide melt (Wirth et al., 2013 and references therein). These factors should be taking into consideration in further studies, along with careful inspection of samples using high-resolution imaging techniques.

An additional aspect that becomes important when evaluating PGE-NPs stability is that post-magmatic alteration processes have affected the Caridad chromite deposit. The fact that Ir-Pt nanoparticles were also found in grains of partly altered pentlandite grains raises the question on the potential effects of alteration processes on the stability of noble metal nanoparticles within the chromite host. It is well known that pentlandite is replaced by secondary heazlewoodite under the reducing conditions that are typical of the initial stages of ocean-floor serpentinization, producing a progressive desulfurization of pentlandite as well as changes in its crystal structure (Klein and Bach, 2009). Under these conditions, it is likely that Ir and Pt nanoparticles may have undergone diffusion-driven modification or coarsening (e.g., Ostwald ripening) due to changes in porosity or phase changes within the sulfide matrix. In contrast, if the Ir-Pt nanocrystals were originally captured by the sulfide melt, the structural changes promoted by the progressive transformation of pentlandite to heazlewoodite during subsolidus re-equilibration or post-magmatic alteration might produce clustering of Ir-Pt nanocrystals along preferential zones (e.g., reaction fronts between pentlandite and heazlewoodite as shown in Fig. 4d). In both contrasting scenarios, the aggregation and coalescence of nanoparticles would produce larger Ir-Pt nanocrystals that may grow to micrometric-sized Ir-Pt grains. Further experimental studies and analytical observations using FIB-FESEM and high-resolution TEM are necessary to confirm this hypothesis. Alternatively, Ir-Pt nanoalloys might result from the dissolution of pre-existing micrometer-sized Ir-Pt alloys by reaction with serpentinization-related fluids (e.g., Fig. 4c), regardless of whether these alloys were formed or not by coalescence of smaller Ir-Pt nanoparticles at higher (magmatic) temperatures. In this third scenario, the interaction of the micron-sized Ir-Pt alloys with low-temperature hydrothermal fluids would result in dissolution and re-precipitation of Ir and Pt alloys to form nanoalloys throughout the pentlandite matrix. Despite it is well known that noble metals are usually immobile under reducing conditions during alteration (Snow and Schmidt, 1998; Rehkämper et al., 1999), highly oxidizing fluids related to the late stages of seafloor weathering (i.e., carbonation) may effectively mobilize PGEs (Fisher et al., 1988). However, little is known about PGE speciation and transport under such conditions (dissolved *vs.* colloidal, or even bacterial effects, e.g., Reith et al., 2016), so additional experiments are necessary to determine the solubility of PGEs in hydrothermal fluids involved in the process of serpentinization.

3.2. Os-Ir-(Ru) nanoparticles in laurite from chromite deposits of the Dobromirtsi Ultramafic Massif (southern Bulgaria): primary origin and effects of retrograde metamorphism

The Late Tertiary Rhodope Metamorphic Core Complex in southern Bulgaria and northern Greece contains numerous slivers of metamorphosed ophiolite complexes. The Dobromirtsi Ultramafic Massif is the largest of these ophiolitic bodies and contains two hundred single chromite bodies, some of them with up to 250,000 tonnes of chromite ore (Payakov et al., 1961; Tarkian et al., 1991; Zhelyaskova-Panayotova and Zinzov, 2000). These chromite deposits were affected by two events of alteration that might be correlated with the exhumation of the Rhodope Metamorphic Core Complex (González-Jiménez et al., 2015a). The first event involved the infiltration of highly reducing fluids during amphibolite facies metamorphism (645–590 °C; 9–6 kbar; 43 Ma), whereas the second was characterized by a change from reducing to oxidizing conditions that took place during the retrograde greenschist-facies overprinting (580–470 °C; 37–35 Ma; Ovtcharova, 2004; Cherneva and Georgieva, 2005). Rims of ferrian chromite were formed on magmatic chromite during the second event, and therefore, the chromite deposits of Dobromirtsi offer a unique opportunity to discuss the potential impacts of retrograde metamorphism on nanoparticle formation and/or de-stabilization.

3.2.1. Primary (magmatic) origin of Os-Ir-(Ru) nanoparticles

In the Dobromirtsi chromite deposits, euhedral nanocrystals of Os-Ir of ~500 nm are often associated with larger (~10 μm) laurite crystals hosted within unaltered cores of chromite grains (Fig. 5a-b), suggesting a primary (magmatic) origin. Empirical and experimental data indicate that laurite can accommodate up to 10 wt% Ir, whereas there is a complete solid solution with Os towards the end member erlichmanite (OsS_2) (Garuti et al., 1999; Brenan and Andrews, 2001; Andrews and Brenan, 2002; González-Jiménez et al., 2009). Brenan and Andrews (2001) and Andrews and Brenan (2002) showed that low Os-Ir laurite (RuS_2) can crystallize from sulfur-undersaturated melts (log fS_2 from −2 to −1.3) in equilibrium with Ru-poor Os-Ir alloys under chromian-spinel liquidus temperature conditions (1200 to 1300 °C). However, the PGM grains synthesized by Brenan and Andrews (2001) and Andrews and Brenan (2002) were larger than 20 μm in diameter, and thus these experiments cannot be extrapolated beyond the microscale (i.e., nanoscale realm). Indeed, the closest approach was given by Bockrath et al. (2004)and Ballhaus et al. (2006), which were able to synthesize submicron crystals of metallic Ir and Ru on surfaces of chromite that crystallized directly from a basaltic melt at high temperatures. Although there are no experimental data for the highly refractory Os, the observation by Ballhaus et al. (2006) that higher melting points of the PGEs correlate with smaller particle sizes of the metallic crystals, allow to suggest that Os would tend to form metal particles with the smallest particle sizes since this element has the highest melting point of the noble metals (T_m ~ 3000 °C). As noted above, early crystallization of chromite from the silicate melt may promote small changes in the local fO_2 conditions of the parental melt, causing the nucleation of nano-sized metallic clusters of PGEs on the margins of chromite grains (Mungall, 2002; Finnigan et al., 2008). Therefore, it is likely that as soon as chromite crystallized from the silicate melt, Os nanoparticles may have been sequestered by the growing spinel. This interpretation is in agreement with the observation that Os alloyed with Ir and not with Ru in the chromite deposits of Dobromirtsi (Fig. 5a-b), suggesting a decoupled geochemical behavior between Ru and Os-Ir in a very early magmatic stage.

Besides the potential effect of the differential incorporation of Os, Ir and Ru within the chromite structure (e.g., Capobianco and Drake, 1990; Righter et al., 2004; Brenan et al., 2012), fractionation betwen Os-Ir and Ru at magmatic temperatures could be the result of a combination of the following factors: (1) Differences in valence states, i.e., Ru was dissolved in the silicate melt as Ru^{4+} (Bockrath et al., 2004; Laurenz

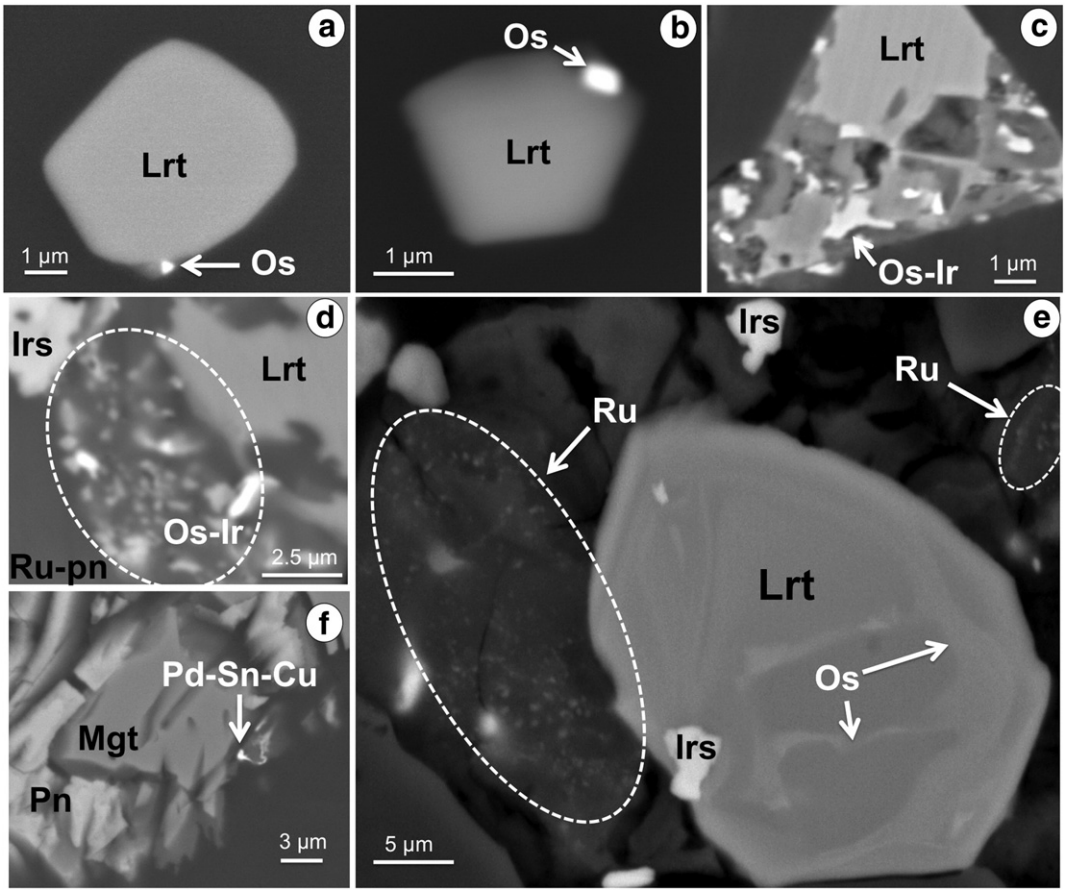

Fig. 5. Backscattered electron images of PGE-NPs associated with micrometric PGM, oxides and sulfides in the chromite deposits of Dobromirtsi (southern Bulgaria), obtained using FESEM. (a–b) are grains included in unaltered chromite grains, (c–d) grains are hosted in altered rims of chromite, and (e–f) are grains located in the interstitial serpentinized silicate matrix between larger chromite grains. Abbreviations: Lrt: laurite (RuS_2), Os-Ir: osmium-iridium alloy, Irs: irasite (IrAsS), Ru-pn: ruthenian pentlandite, Pn: pentlandite, Mgt: pentlandite, Ru: native ruthenium.

et al., 2013) whereas Os and Ir were dissolved as trivalent and divalent species, respectively; (2) Variation of the Ru/(Os + Ir) ratio in the melt, attributed to partial dissolution of PGMs and/or clusters of metallic Ru and/or Os-Ir alloys (Fonseca et al., 2012), resulting from variable degrees of partial melting of peridotite-hosted base-metal sulfides containing PGEs in solid solution as well as nano- to micron-sized PGM (including alloys, sulfides, arsenides, bismuthides and tellurides) associated with them (Lorand et al., 2010; Alard et al., 2011; Luguet et al., 2007; Kogiso et al., 2008; Marchesi et al., 2011; González-Jiménez et al., 2014; Aulbach et al., 2016; O'Driscoll and González-Jiménez, 2016; Wainwright et al., Submitted for publication); and (3) Nanoscale surface effects, e.g., preferred metal-ligand association of Ru (i.e., Ru-S) relative to metal-metal bonding of Os and Ir (i.e., Os-Ir).

Interestingly, Finnigan et al. (2008) reported Ru-S nanoparticles of ~250 nm in their experiments, whereas Bockrath et al. (2004) suggested an average size of ~290 nm for the formation of stable Ru metal nuclei. Despite the fact that micrometer-sized crystals of laurite (RuS_2) have been osbserved to crystallize directly from silicate melts (Andrews and Brenan, 2002; Fonseca et al., 2012), the occurrence of precursor nanoscale phases (e.g., polycrystalline aggregates of Ru-S (and Ru metal) clusters) would facilitate nucleation and growth of micron-size laurite crystals. Indeed, PGE-NPs may represent the very first stage of PGM nucleation, as suggested by Baumgartner et al. (2013) and Helmy et al. (2013). Therefore, many laurites in natural chromite deposits may have formed by aggregation or aglomeration of clusters of pre-existing Ru-S nanoparticles and/or Ru that have reacted with S, rather than forming as a liquidus phase that crystallized directly from a sulfur-bearing, sulfide-undersatured silicate melt (Bockrath et al., 2004).

In a potential scenario where Os-Ir (nano) alloys may have been segregated before and/or separately of laurite from the basaltic melt (and/or inherited after exhaustion of PGE-bearing BMS), it is likely that these nanoparticles were entrapped into the growing sulfide matrix and become "invisible" to conventional SEM and EMPA observation. This may explain the common presence of Os-(Ir)-rich laurites in chromite deposits elsewhere (Garuti et al., 1999; González-Jiménez et al., 2009). "Invisible" or refractory precious metals such as Au are common in sulphides from magmatic-hydrothermal ore deposits including Carlin-type, orogenic and epithermal Au deposits, to name a few. In these ores, Au occurs in Au-rich patches and overgrowths in arsenian pyrite ($Fe(S,As)_2$), as detected using EMPA, SIMS and LA-ICP-MS techniques (concentration range from a few ppm to up to wt% levels; Deditius et al., 2014) (see BSE image of pyrite grain in Fig. 1, bottom). Spectroscopic (XANES) and electron microscopy (TEM) studies have demonstrated that in these Au-rich areas Au can occur in solid solution (Au^{+1}) or most notably, forming clusters of discrete nanoparticles of native Au (~5–10 nm) that are "invisible" in SEM/EMPA-BSE images (Palenik et al., 2004; Reich et al., 2005, 2006; Deditius et al., 2014; Hough et al., 2012).

3.2.2. Effects of retrograde metamorphism on Os-Ir-(Ru) nanoparticle stabiliy

In the altered zones of the Dobromirtsi chromite deposits, partly altered laurites contain nanometer-sized Os-Ir alloys at the grain margins or boundaries (Fig. 5c). These nanoparticles are also observed along the interface between secondary Ru-pentlandite and partly altered laurite (Fig. 5d). Moreover, clusters of nm-sized particles of Os-Ir define an irregular zoning in one laurite grain located in the interstitial matrix

(Fig. 5e). Interestingly, the Fe-oxide matrix surrounding this irregularly zoned laurite grain is dusted with a myriad of native Ru (Ru^0) nanoparticles (Fig. 5e). Finally, two grains of a Pd-Sn-Cu nanomineral are attached to the rims of magnetite replacing a partly desulfurized pentlandite in the serpentinized silicate matrix in these chromite deposits (Fig. 5f). This raises the question whether the occurrence of PGE-NPs in altered laurites within chromite is not only dependent on the thermodynamic stability of the PGE-NPs themselves (as isolated entities), but also result from more complex nanoparticle-mineral host interactions during alteration of the latter.

González-Jiménez et al. (2010) showed that during the first metamorphic stage affecting the Dobromirtsi chromite deposits some primary (magmatic) laurites were reworked under low fO_2 (and fS_2), which has caused their partial desulfurization and corrosion. Considering that Os and Ir could be initially dissolved heterogeneously in solid solution or contained as PGE-NPs in laurite, the metamorphic changes affecting the structure of the host sulfide may have induced segregation of these elements as metal nanoparticles (e.g., Fig. 5c). In contrast, reaction of laurite with metamorphic-hydrothermal fluids progressively higher in fO_2 (and fS_2) has caused a transformation of laurite to more complex assemblages containing Ru-rich base metal sulfides + Os-Ir nanoalloys (González-Jiménez et al., 2010). This reaction involved the transformation of laurite, first, to a metastable Ru-rich monosulfide solid solution that is subsequently re-equilibrated into Ru-rich pentlandite at a temperature of ~500 °C. It appears that during this reaction, Os and Ir are released preferentially along the reaction fronts (Fig. 5d). The fact that pentlandite may accommodate relatively high contents of Ru in solid solution (up to 12.9 wt%; Mackovicky et al., 1986) but very low of Os and Ir provides a clear example of fractionation between Os-Ir and Ru at moderate temperatures.

A complete reaction of desulfurization of pre-existing laurite under low fO_2 (and fS_2) conditions may also explain the formation of Ru^0 nanoparticles in the oxide matrix surrounding the laurite grain shown in Fig. 5e. In this case, Ru^0 must have been accumulated in the residual oxide matrix once all the elemental components of laurite were lost. In contrast, the irregular zoning of this grain and its highly radiogenic $^{187}Os/^{188}Os$ signature suggest additional re-equilibration with oxidizing fluids carrying Os. Experiments conducted at 500 °C indicate that Os uptake in pyrite can only occur by step-growth processes (Brenan et al., 2000). Consequently, at such temperatures the only way to disturb Os isotopic exchange in laurite is via dissolution/precipitation. Therefore, segregation of nanoclusters of Os-Ir alloys is less likely to have occurred by simple solid-state diffusional process. This interpretation may also apply for the very small particles of Pd-Sn-Cu attached to magnetite replacing pentlandite in the serpentinized matrix of one chromite deposit at Dobromirtsi. At the given temperatures Pd is more soluble and can be more easily transported than the other PGEs by a variety of complexes that include chloride, hydroxide and bisulfide species (Wood, 2002). However, the possibility of physical (or colloidal) transport of Pd and other precious metals in hydrothermal-metamorphic fluids remain speculative and has not been explored yet.

3.3. Ru-(Os-Ir) mineral nanoparticles in laurites from the Loma Baya chromite deposit (southwestern Mexico): effects of thermal metamorphism

González-Jiménez et al. (2015b) carried out a detailed study on the chromite alteration and the stability of Ru-Os-Ir nanoparticles in the Loma Baya chromite deposit in Mexico. The Loma Baya ores are a series of small bodies of massive chromitite reaching total resources of ~ 28,000 Mt of chromite that were exploited for Cr during the late 1980s (Salgado-Terán and Serrano-Villar, 1983). The Loma Baya ultramafic complex represents a portion of obducted sub-arc mantle, which probably formed in an intra-oceanic island arc developed during Late Jurassic to Early Cretaceous time along the paleo-Pacific coast of Mexico (Mendoza, 2000; Mendoza and Suastegui, 2000; Ortiz-Hernández et al., 2006). The Loma Baya ultramafic rocks and their hosted chromite deposit underwent an early hydrous metamorphism phase (greenschist-to-blueschist facies, T = 200–330 °C and P = 0.5–0.7 GPa), followed by a dehydration event related to the intrusion of mid-Tertiary granites (Mendoza and Suastegui, 2000). Hence, these rocks provide a unique opportunity to compare the effects of thermal metamorphism on the composition of chromite and to explore how changes in temperature and variable degrees of fluid-rock interaction can impact the distribution of PGEs within chromite-hosted IPGE carrier phases (González-Jiménez et al., 2015b). In this section we summarize their descriptions and interpretation and discuss the potential effects of thermal metamorphism on the fate PGE-NPs in natural samples.

The metamorphic rims of chromite and the interstitial chlorite matrix between chromite grains host Ru-(Os-Ir) nanocrystals as inclusions in partly desulfurized laurites (Fig. 6a-f). The distribution mode and sizes of the PGE-NPs is related with the internal microstructure of the laurite pseudomorph (Fig. 6a-f). Thus, laurite pseudomorphs with micrometer-sized pores and/or a dense fracture network contain abundant Ru-(Os-Ir) nanoparticulate alloys with rounded shapes, with average diameters of ~110 nm and modal abundances of ~60 nm (Fig. 6a-b). In contrast, laurite pseudomporh whose proportion of pores are much lower display zoning defined by homogenous nanoparticle-free S-deficient cores or rims (concentric or irregular, patchy zones) alternating with zones that contain abundant Ru-(Os-Ir) nanocrystals. These PGE-NPs have average diameters of ~110 nm and ~90 nm, respectively (Fig. 6c-d). In a third type of laurite pseudomorph, where micrometer-sized pores are rare or absent, the Ru-(Os-Ir) nanocrystals clump to form particle aggregates with variable average sizes (Fig. 6e-f). In the latter grains the size distribution is bimodal with abundant particles smaller than 100 nm, which coexist with a few larger ones (~500 nm).

González-Jiménez et al. (2015b) suggested that the segregation of the Ru-(Os-Ir) nanocrystals was a consequence of the textural and structural rearrangement of magmatic laurite during metamorphism. These authors suggested that during the first stage of hydrous metamorphism under greenschist-to-blueschist facies conditions (200–300 °C), the infiltration of sulfur-poor fluids caused the desulfurization of laurite. Volume changes associated with the reduction of the original sulfide grain at subsolidus conditions resulted in the formation of nanoporosity and an interconnected network of fractures within laurite. These structural changes in the mineral structure promoted diffusional processes, triggering the segregation of the Ru-(Os-Ir) nanoparticles of < 10 nm (Fig. 6a-b). However, this simplified trajectory does not satisfactorily explain the different degrees of porosity of the laurite matrices and the broad Ru-(Os-Ir) nanoparticle size distributions (from tens of nm to 1 μm). González-Jiménez et al. (2015b) suggested that the observed differences in the microstructures of laurite and the range of sizes of the noble-metal nanocrystals could be the result of heating associated with the thermal metamorphism that affected the Loma Baya chromite deposit.

González-Jiménez et al. (2015b) recently compiled data sets on noble metal nanoparticles to provide a first attempt to constrain PGE-NPs thermal stability in laurite. Based on available experimental data, the authors constructed a plot of temperature *vs.* particle size for Ru-(Os-Ir) nanoparticles enclosed in laurite-type mineral host that matches well with the rsults from *in situ* heating TEM experiments of Reich et al. (2006). Using the Au-FeS_2 system as analogue — laurite (RuS_2) has a pyrite-type structure and the bulk melting temperature of Au (1064 °C) does not differ significantly from Ru-(Os-Ir) alloys (~1300 °C) — González-Jiménez et al. (2015b) argued that Ru-(Os-Ir) nanoparticles that were previously exsolved during hydrous metamorphism from homogeneous magmatic laurites (trajectory 2 ⇒ 3 in Fig. 7b) underwent a prograde path from ~300 °C to 550–560 °C as a result of thermal metamorphism (trajectory 3 ⇒ 4 ⇒ 5 in Fig. 7b). This dramatically affected nanoparticle stability, promoting coarsening by diffusion-driven, solid state Ostwald ripening (trajectory 3 ⇒ 4 in Fig. 7b), as observed during *in situ* TEM heating by Reich et al. (2006). Considering that such prograde heating (and further cooling) affected

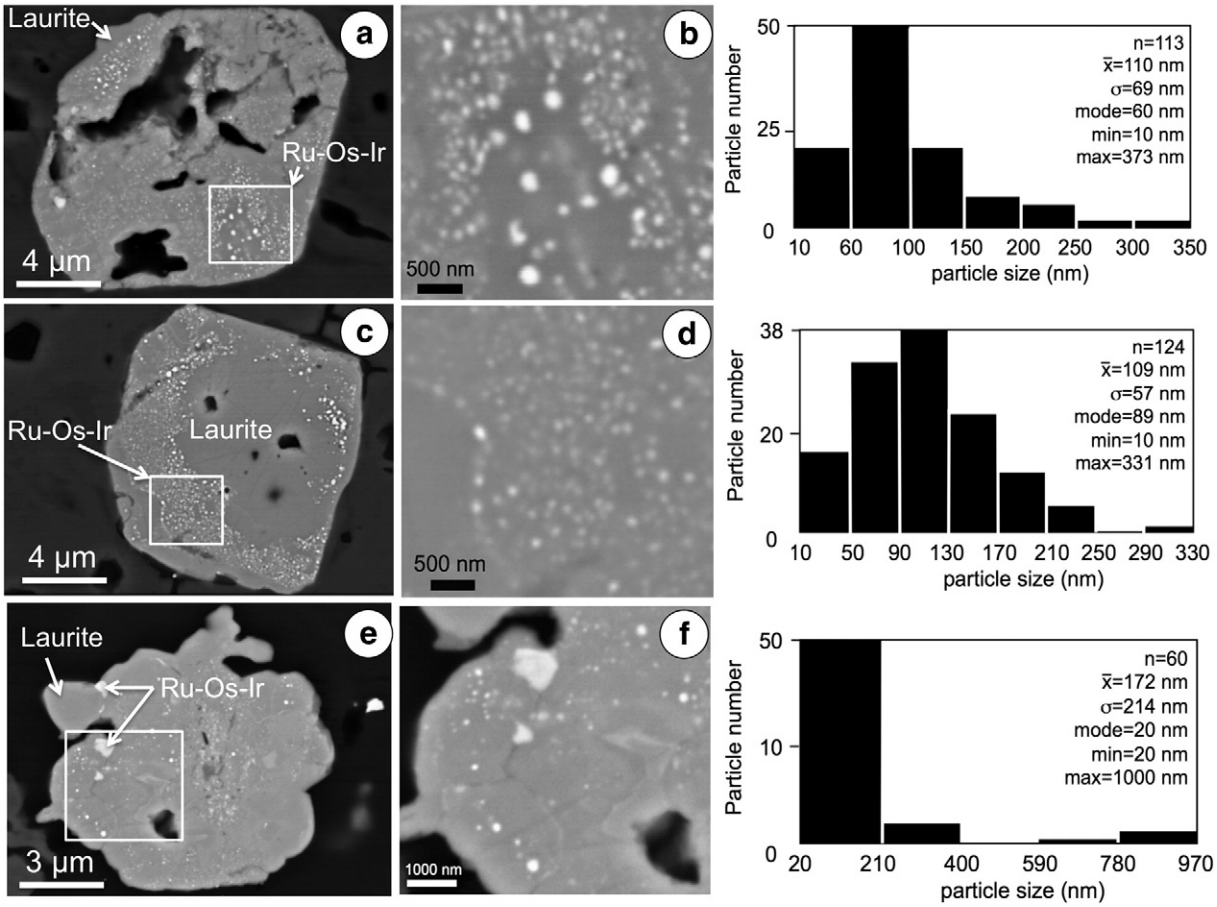

Fig. 6. Backscattered electron images obtained using FESEM of PGE-NPs in partly altered laurite grains from the chromite deposit of Loma Baya in southwestern Mexico (González-Jiménez et al., 2015b). Details of the nanoparticles enclosed by the squares are shown on the left side of the images together with their particle size distribution.

the host rocks differentially as function of the distance to the heat source (trajectories 5 ⇒ 6⇒ 7 ⇒ 8, and 5 ⇒ 9 in Fig. 7b), it is likely to expect a wide spectrum of Ru-(Os-Ir) particle sizes and textures, as observed at Loma Baya (Fig. 6). These data suggest that thermal events can have an unforessen impact on PGE nanoparticle stability, and thus may impact the PGE tenor of chromite deposits

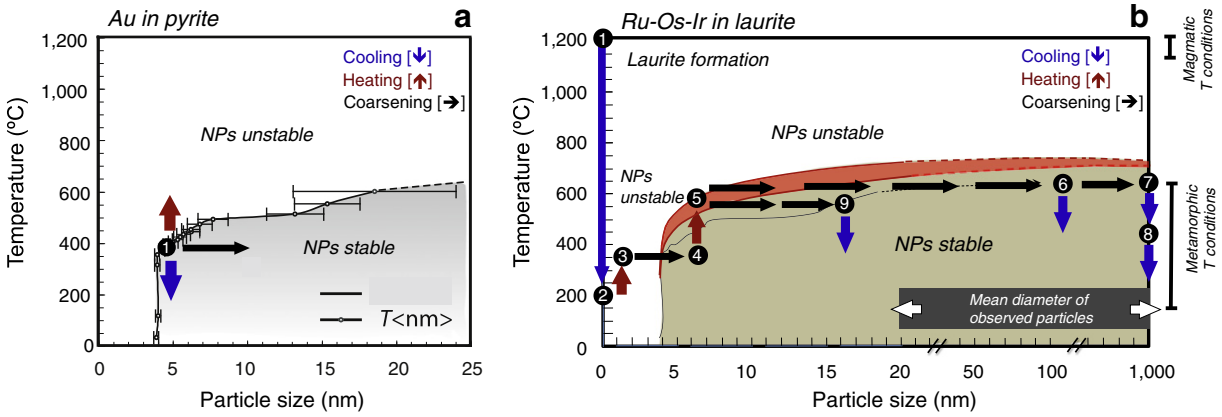

Fig. 7. Thermal effects on noble metal nanoparticle stability as a function of particle size. (a) *In situ* TEM heating experiments showing the effect of nanoparticle-mineral host interaction during the thermal evolution of native Au nanoparticles contained in arsenian pyrite. The black (coarsening) curve shows the temperature of complete dissolution of Au^0 nanoparticles in arsenian pyrite, plotted as the average diameter of the particle-size distribution (circles with standard error bars) for a given temperature. For the case of a particle size distribution of ~5 nm at T~400 °C (black circle labeled "1"), Au^0 nanoparticles remain stable during cooling (blue arrow). In constrast, if the particles are heated above this temperature, they will be de-stabilized and will dissolve into the sulfide (red arrow) unless coarsening occurs (black horizontal arrow). Figure modified from Reich et al. (2006). (b) Temperature *vs.* particle size stability diagram for Ru-(Os-Ir) nanoparticles in a laurite-type host (after González-Jiménez et al., 2015b). The thick red curve represents the nanoparticle-coarsening boundary. Above this upper temperature limit (e.g., point 5), Ru-(Os-Ir) nanoparticles in laurite are unstable unless coarsening occurs (black horizontal arrows). The lower light brown field represents the temperature *vs.* particle size range of stability of nanoalloys (NPs stable).

4. Conclusions

Previously published experimental studies and observations in natural samples suggest that the PGE budget of some magmatic PGE-(Cr) deposits may not be exclusively associated to the presence of micrometric PGMs or in solid solution in the base-metal sulphides (BMS). Alhough often overlooked, platinum-group element nanoparticles (PGE-NPs) could be more frequent in these ores than previously thought. Based on the evidence reviewed in this paper, there is a need for further high-resolution observations aimed at detecting PGE-NPs, and the recent development of analytical techniques for imaging and characterization using combination of FIB and TEM methods opens a new avenue of research.

Previously published studies at the Bushveld Complex in South Africa (e.g., Wirth et al., 2013 and Junge et al., 2015) and the Caridad Mine in Cuba we have documented here suggest that PGE-NPs might precede the segregation of immisicible sulfide liquids in the magmatic source. This might be also supported by experimental data by Helmy et al. (2013), although more studies are needed to support such intepretation. The segregation of PGE-NPs at shallower levels of the lithosphere could be promoted by changes in the activity of silica ($a SiO_2$) and/or oxygen fugacity (fO_2) as soon as mineral such olivine and/or chromite crystallize early in the basaltic melt. Once sulfide saturation is achieved, these PGE-NPs may be entrained or captured by the sulfide liquid, producing PGE-rich sulfide melts. Upon cooling, these sulfide liquids solidify as monosulfide solid solution (mss), while further cooling may promote subsolidus requilibration of the *mss* to produce a series of base-metal sulfides (i.e., pentlandite, chalcopyrite or bornite). It is likely that structural changes associated with polymorphic reactions of phase transformation may favour the formation of secondary PGE-NPs (from primary nanoparticles, or due to diffusion of PGEs from the matrix), despite the fact that a dominant proportion of PGEs may still be retained in solid solution within the structure of the host sulfides. In this context, chromite may play the role of a trigger for metal nanoparticle nucleation from PGEs originally dissolved in the silicate melt. Either captured by immisicible sulfide liquids or oxide/sulfide mineral phases, physical fractionation provides a complementary (or alternative) mechanism to explain the effective fractionation of PGEs from silicate melts into PGE-rich ores. This is in agreement with previous suggestions that PGE fractionation under high temperature (magmatic) conditions may be controlled not only by the chemical propierties of PGEs (e.g., solubility, speciation, etc.) but also by surface kinetic effects and/or nanoscale phenomena arising at the mineral-melt interface. Nevertheless, further experimental studies and high-resolution observations in natural samples are necessary in order to better understand PGE partitioning under these conditions.

During the formation of chromitites by mixing of melts within conduits in the upper mantle or in crustal chambers (e.g., chromite layers or reef of the Buhsveld complex), changes in fO_2 (apart from the reduction promoted by chromite growth), fS_2 and Ru/(Os + Ir) ratios can promote different scenarios favouring the fractionation between Os-Ir-Ru and Pt-Pd. It is likely that PGE fractionation may be related to the formation of different types of PGE-NPs that have crystallized under different conditions from the melt, and characterized by different particle sizes. The experimental results by Helmy et al. (2013) allow us to suggest that different metal-ligands complexes or atomic clusters could play an important role in stabilizing PGE-NPs under magmatic conditions.

The preservation and modification of primary (magmatic) PGE-NPs during retrograde (cooling) or prograde (heating) metamorphism is a relevant aspect that must be addressed in future studies. For example, the identification of the same suites of PGE-NPs in sulfide minerals (i.e., pentlandite and laurite) in unaltered and altered zones of the chromite deposits of Caridad (eastern Cuba) ad Dobromirtsi (southern Bulgaria) raises the question about the magmatic origin of the PGE-NPs (>1000 °C), and their fate at low temperature. In some cases, the PGE-NPs are found in replacement/reaction fronts of the primary sulfides to secondary sulfides or oxides, strongly suggesting that PGE-NPs can also form under low temperature conditions (<200–600 °C). This is particularly evident in the case of Ru^0 nanoparticles that occur in association with secondary oxides at the Dobromirtsi chromite deposits in Bulgaria. These case studies give examples of how PGE-NPs can eventually form under a wide spectrum of temperature (and pressure) conditions, and provide evidence that hydrothermal fluids play a relevant role in producing PGE-NPs during retrograde metamorphism. Finally, results from the Loma Baya deposits in Mexico show that heating events (e.g., prograde and contact metamorphism) can also affect chromite deposits that have undergone retrograde alteration. In this particular case, heating and dehydration promoted coarsening of PGE-NPs to sizes larger than a micron. These effects are consistent with heating experiments of gold in pyrite and may offer an alternative explanation for the formation of secondary micron-size PGM alloys derived from the alteration of PGE-bearing sulfides.

Acknowledgements

This research was financially supported by the MSI grant "Millenium Nucleus for Metal Tracing along Subduction" (NC130065). Additional funding was provided to J.M. González-Jiménez through the Fondecyt Initiation Grant #11140005 "Decoding precious metals (platinum-group elements and gold) in upper mantle rocks of the Chilean Coastal Cordillera".

References

Alard, O., Lorand, J.-P., Reisberg, L., Bodinier, J.-L., Dautria, J.M., O'Reilly, S.Y., 2011. Volatile-rich metasomatism in Montferrier xenoliths (southern France): consequences for chalcophile and highly siderophile elements abundances in the sub-continental mantle. J. Petrol. 52, 2009–2045.

Andrews, D.R.A., Brenan, J.M., 2002. Phase-equilibrium constraints on the magmatic origin of laurite + Ru–Os–Ir alloy. Can. Mineral. 40, 1705–1716.

Arndt, N.T., Lesher, C.M., Czamanske, G.K., 2006. Mantle-derived magmas and magmatic Ni-Cu-(PGE) deposits. In: Hedenquist, J.W., Thompson, J.F.H., Goldfarb, R.J., Richards, J.P. (Eds.), Economic geology—one hundredth anniversary volume 1905–2005: Littleton. Colorado, Society of Economic Geologists, pp. 5–23.

Aulbach, S., Mungall, J.E., Pearson, D.G., 2016. Distribution and processing of highly siderophile elements in cratonic mantle lithosphere. Rev. Mineral. Geochem. 81, 239–304.

Ballhaus, C., Ulmer, P., 1995. Platinum-group elements in the Merensky reef: II. experimental solubilities of platinum and palla- dium in $Fe_{1-x}S$ from 950 to 450 °C under controlled fS_2 and fH_2. Geochim. Cosmochim. Acta 59, 4881–4888.

Ballhaus, C., Sylvester, P., 2000. PGE enrichment processes in the Merensky reef. J. Petrol. 41, 454–561.

Ballhaus, C., Tredoux, M., Späth, A., 2001. Phase relations in the Fe-Ni-Cu-PGE-S system at magmatic temperatura and application to massive sulphide ores of the Sudbury Igneous Complex. J. Petrol. 42, 1911–1926.

Ballhaus, C., Bockrath, C., Wohlgemut-Ueberwasser, C., Laurenz, V., Berndt, J., 2006. Fractionation of the noble metals by physical processes. Contrib. Mineral. Petrol. 152, 667–684.

Banfield, J.F., Navrotsky, A. (Eds.), 2001. Nanoparticles and the Environment. Rev. MinerGeochem 44. Mineralogy Society of America, Chantilly, VA (349 pp).

Barnes, S.-J., Ripley, E.M., 2016. Highly siderophile and strongly chalcophile elements in magmatic ore deposits. Rev. Mineral. Geochem. 81, 725–774.

Baumgartner, J., Dey, A., Bomans, P.H., Le Coadou, C., Fratzl, P., Sommerdijk, N.A., Faivre, D., 2013. Nucleation and growth of magnetite from solution. Nat. Mater. 12, 310–314.

Bockrath, C., Ballhaus, C., Holzheid, A., 2004. Stabilities of laurite RuS_2 and monosulphide liquid solution at magmatic temperature. Chem. Geol. 208, 265–271.

Borisov, A., Nachtweyh, K., 1998. Ru solubility in silicate melts: experimental results in oxidizing region. Lunar and Planetary Science XXIX, Abstract 1320.

Borisov, A., Palme, H., 1995. The solubility of iridium in silicate melts: new data from experiments with Ir10Pt90 alloys. Geochim. Cosmochim. Acta 57, 481–485.

Borisov, A., Palme, H., 1997. Experimental determination of the solubility of platinum in silicate melts. Geochim. Cosmochim. Acta 61, 705–716.

Borisov, A., Palme, H., 2000. Solubility of noble metals in Fe-containing silicate melts as derived from experiments in Fe free systems. Am. Mineral. 85, 1665–1673.

Borisov, A., Walker, R.J., 2000. Os solubility in silicate melts: new efforts and results. Am. Mineral. 85, 912–917.

Borisov, A., Palme, H., Spettel, B., 1994. Solubility of palladium in silicate melts: implications for core formation in the Earth. Geochim. Cosmochim. Acta 58, 705–716.

Brenan, J.M., Andrews, D., 2001. High-temperature stability of Laurite and Ru–Os–Ir alloy and their role in PGE fractionation in mafic magmas. Can. Mineral. 39, 341–360.

Brenan, J.M., Cherniak, D.J., Rose, L.A., 2000. Diffusion of osmium in pyrrhotite and pyrite: implications for closure of the Re-Os isotopic system. Earth Planet. Sci. Lett. 180, 399–413.

Brenan, J.M., Finnigan, C.F., McDonough, W.F., Homolova, V., 2012. Experimental constraints on the partitioning of Ru, Rh, Ir, Pt and Pd between chromite and silicate melt: the importance of ferric iron. Chem. Geol. 302-303, 16–32.

Cabri, L.J., 2002. The platinum-group minerals. In: Cabri, L.J. (Ed.), The Geology. Geochemisty, Mineralogy and Mineral Beneficiation of Platinum-Group elements.

Campbell, I.H., Naldrett, A.J., Barnes, S.J., 1983. A model for the origin of platinum-rich sulphide horizons in the Bushveld and Stillwater complexes. J. Petrol. 24, 133–165.

Capobianco, C.J., Drake, M.J., 1990. Partitioning of ruthenium, rhodium, and palladium between spinel and silicate melt and implications for platinum-group element fractionation trends. Geochim. Cosmochim. Acta 54, 869–874.

Cherneva, Z., Georgieva, M., 2005. Metamorphosed Hercynian granitoids in the Alpine structures of the Central Rhodope, Bulgaria: geotectonic position and geochemistry. Lithos 82, 149–168.

Ciobanu, C.L., Cook, N.J., Pring, A., Brugger, J., Danushevsky, L., Shimizu, M., 2009. 'Invisible gold' in bismuth chalcogenides. Geochim. Cosmochim. Acta 73, 1970–1999.

Ciobanu, C.L., Cook, N.J., Utsunomiya, S., Pring, A., Green, L., 2011. Focussed ion beam - transmission electron microscopy applications in ore mineralogy: bridging micron- and nanoscale observations. Ore Geol. Rev. 42, 6–31.

Ciobanu, C.L., Cook, N.J., Utsunomiya, S., Kogagwa, M., Green, L., Gilbert, S., Wade, B., 2012. Gold-telluride nanoparticles revealed in arsenic-free pyrite. Am. Mineral. 97, 1515–1518.

Deditius, A., Utsunomiya, Reich, M., Kesler, S.E., Ewing, R.C., Hough, R., Walshe, E.J., 2011. Trace metal nanoparticles in pyrite. Ore Geol. Rev. 42, 32–46.

Deditius, A., Reich, M., Kesler, S.E., Utsunomiya, S., Chryssoulis, S., Walshe, J.L., Hough, R., Ewing, R.C., 2014. The coupled geochemistry of Au and As in pyrite from hydrothermal ore deposits. Geochim. Cosmochim. Acta 140, 644–670.

Ertel, W., O'Neill, H.S.C., Sylvester, P.J., Dingwell, D.B., 1999. Solubilities of Pt and Rh in haplobasaltic silicate melt at 1300°C. Geochim. Cosmochim. Acta 63, 2439–2449.

Finnigan, C.S., Brenan, J.M., Mungall, J.E., McDonough, W.F., 2008. Experiments and models bearing on the role of chromite as a collector of platinum group minerals by local reduction. J. Petrol. 49, 1647–1665.

Fisher, W., Amossé, J., Leblanc, M., 1988. PGE Distribution in some Ultramafic Rocks and Minerals from the Bou-Azzer Ophiolite Complex (Morocco). In: Potts, P.J., Bowles, J.F.W., Cribb, S.J. (Eds.), Geo-Platinum Sympoisium. Vol. (H.M. Prichard. Elsevier, London, pp. 199–210.

Fonseca, R.O., Mallmann, G., O'Neill, H.S.C., Campbell, I.H., Laurenz, V., 2011. Solubility of Os and Ir in sulfide melt: implications for Re/Os fractionation during mantle melting. Earth Planet. Sci. Lett. 311, 339–350.

Fonseca, R.O.C., Laurenz, V., Mallmann, G., Luguet, A., Hoehne, N., Jochum, K.P., 2012. New constrains on the genesis and long-term stability of Os-rich alloys in the Earth's mantle. Geochim. Cosmochim. Acta 87, 277-242.

Fortenfant, S.S., Dingwell, D.B., Ertel-Ingrisch, W., Capmas, F., Birk, J.L., Dalpe, C., 2006. Oxygen fugacity dependence of Os solubility in haplobasaltic melt. Geochim. Cosmochim. Acta 70, 742–756.

Garuti, G., Zaccarini, F., Economou-Eliopoulos, M., 1999. Paragenesis and composition of laurite from chromitites of Othrys (Greece): implications for Os–Ru fraction- ation in ophiolitic upper mantle of the Balkan peninsula. Mineral. Deposita 34, 312–319.

Gervilla, F., Leblanc, M., 1990. Magmatic ores in high-temperature Alpine-type lherzolite massifs (Ronda, Spain and Beni Bousera, Morocco). Econ. Geol. 85, 112–132.

Gervilla, F., Proenza, J.A., Frei, R., González-Jiménez, J.M., Garrido, C., Melgarejo, J.C., Meibom, A., Díaz-Martínez, R., Lavaut, W., 2005. Distribution of platinum-group elements and Os isotopes in chromite ores from Mayarí-Baracoa Ophiolitic Belt (eastern Cuba). Contrib. Mineral. Petrol. 150, 589–607.

Godel, B., Barnes, S.-J., Maier, W.D., 2007. Platinum-group elements in sulphide minerals, platinum-group minerals, and whole-rock of the Merensky Reef (Buhsveld Complex, South Africa): implications for the formation of the reef. J. Petrol. 48, 1569–1604.

González-Jiménez, J.M., Gervilla, F., Proenza, J.A., Augé, T., Kerestedjian, T., 2009. Distribution of platinum-group minerals in ophiolitic chromitites. Appl. Earth Sci. 118, 101–110.

González-Jiménez, J.M., Gervilla, F., Kerestedjian, T., Proenza, J.A., 2010. Alteration of platinum-group and base-metal mineral assemblages in ophiolite chromitites from the Dobromirtsi Massif, Rhodope Mountains (Bulgaria). Resour. Geol. 60, 315–334. http://dx.doi.org/10.1111/j.1751-3928.2010.00138.x.

González-Jiménez, J.M., Proenza, J.A., Gervilla, F., Melgarejo, J.C., Blanco-Moreno, J.A., Ruiz-Sánchez, R., Griffin, W.L., 2011. High-Cr and high-Al chromitites from the Sagua de Tánamo district, Mayarí-Cristal Ophiolitic Massif (eastern Cuba): constraints on their origin from mineralogy and geochemistry of chromian spinel and platinum-group elements. Lithos 125, 101–121.

González-Jiménez, J.M., Gervilla, F., Griffin, W.L., Proenza, J.A., Augé, T., O'Reilly, S.Y., Pearson, N.J., 2012. Os-isotope variability within sulfides from podiform chromitites. Chem. Geol. 291, 224–235.

González-Jiménez, J.M., Griffin, W.L., Gervilla, F., Proenza, J.A., O'Reilly, S.Y., Pearson, N.J., 2014. Chromitites in ophiolites: how, where, when, why? Part I. A review and new ideas on the origin and significance of platinum-group minerals. Lithos 189, 127–139. http://dx.doi.org/10.1016/j. lithos.2013.06.016.

González-Jiménez, J.M., Locmelis, M., Belousova, E., Griffin, W.L., Gervilla, F., Kerestedjian, T., O'Reilly, S.Y., Sergeeva, I., Pearson, N.J., 2015a. Genesis and tectonic implications of podiform chromitites in the metamorphosed Ultramafic Massif of Dobromirtsi (Bulgaria). Gondwana Res. 27, 555–574.

González-Jiménez, J.M., Reich, M., Camprubí, T., Gervilla, F., Griffin, W.L., Colás, V., O'Reilly, S.Y., Proenza, J.A., Pearson, N.J., Centeno-García, E., 2015b. Thermal metamorphism of mantle chromites and the stability of noble-metal nanoparticles. Contrib. Mineral. Petrol. 170, 15.

Hanley, R.S., 2007. The role of arsenic-rich melts and mineral phases in the development of high grade Pt-Pd mineralization within komatiite-associated magmatic Ni-Cu sulfide horizons at Dundonald Beach South, Abitibi subprovince, Ontario. Canada. Econ. Geol. 102, 303–315.

Hannington, M., Haroardóttir, V., Garbe-Shönberg, D., Brown, K.L., 2016. Gold enrichment in active geothermal systems by accumulating colloidal suspensions. Nat. Geosci. 9, 299–302.

Helmy, H.M., Ballhaus, C., Fonseca, R.O.C., Wirth, R., Nagel, T., Tredoux, M., 2013. Noble metal nanoclusters and nanoparticles precede mineral formation in magmatic sulphide melts. Nat. Commun. http://dx.doi.org/10.1038/ncomms3405.

Hochella, M.F. Jr., 2002. There's plenty of room at the bottom: nanoscience in geochemistry. Geochim. Cosmochim. Acta 66, 735–743.

Hochella, M.F. Jr., 2008. Nanogeoscience: from origins to cutting-edge applications. Elements 4, 373–379.

Holwell, D.A., Keays, R.R., McDonald, I., Williams, M.R., 2015. Extreme enrichment of Se, Te, PGE and Au in Cu sulfide microdroplets: evidence from LA-ICP-MS analysis of sulphides in the Skaergaard Intrusion, east Greenland. Contrib. Mineral. Petrol. 170 (53).

Hough, R.M., Noble, R.R.P., Hitchen, G.J., Hart, R., Reddy, S.M., Saunders, M., Clode, P., Vaughan, D., Lowe, J., Anand, R.R., Butt, C.R.M., Verrall, M., 2008. Naturally occurring gold nanoparticles and nanoplates. Geology 36, 571–574.

Hough, R., Reich, M., Noble, R., 2012. In: Barnard, A.S., Guo, H. (Eds.), Noble Metal Nanoparticles in Ore Systems. *In:* In Nature's Nanostructures. Pan Stanford Publishing Pte. Ltd., pp. 141–167 (ISBN 978-981-4316-82-8).

Junge, M., Wirth, R., Oberthür, R., Melcher, F., Schreiber, A., 2015. Mineralogical siting of platinum-group elements in pentlandite from the Bushveld Complex. South Africa. http://dx.doi.org/10.1007/s00126-014-0561-0.

Klein, F., Bach, W., 2009. Fe–Ni–Co–O–S phase relations in peridotite- seawater interactions. J. Petrol. 50, 37–59.

Kogiso, T., Suzuki, K., Suzuki, T., Uesugi, K., 2008. Two- and three-dimensional imaging of platinum-group minerals at submicrometer scale with synchrotron X-ray. Goldschmidt Conference Abstracts 2008, p. 1212 (www.minersoc.org).

Laurenz, V., Fonseca, R.O., Ballhaus, C., Jochum, K.P., Heuser, A., Sylvester, P.J., 2013. The solubility of palladium and ruthenium in picritic melts: 2. The effect of sulfur. Geochim. Cosmochim. Acta 108, 172–183.

Leblanc, M., Gervilla, F., Jedwab, J., 1990. Noble metals segregation and fractionation in magmatic ores from Ronda and Beni Bousera lherzolite massifs (Spain, Morocco). Mineral. Petrol. 42, 233–248.

Lee Penn, R., 2012. Uncovering the physical and chemical properties of minerals and mineral nanoparticles. In: S., A., Barnard, L., Guo, H. (Eds.), *:* In Nature's Nanostructures. Pan Stanford Publishing Pte. Ltd., pp. 45–73 (ISBN 978-981-4316-82-8).

Lee, M., 2010. Transmission electron microscopy (TEM) of earth and planetary materials: a review. Mineral. Mag. 74, 1–27.

Lorand, J.-P., Alard, O., Luguet, A., 2010. Platinum-group element micronuggets and refertilization process in Lherz orogenic peridotite (northeastern Pyrenees, France). Earth Planet. Sci. Lett. 289, 298–310.

Luguet, A., Shirey, S.B., Lorand, J.-P., Horan, M.F., Carlson, W., 2007. Residual platinum-group minerals from highly depleted harzburgites of the Lherz massif (France) and their role in HSE fractionation of the mantle. Geochim. Cosmochim. Acta 71, 3082–3097.

Makovicky, M., Makovicky, E., Rose-hansen, J., 1986. Experimental studies on the solubility and distribution of platinum-group elements in base-metal sulphides in platinum deposits. In: Gallagher, M.J., Ixer, R.A., Neary, C.R., Prichard, H.M. (Eds.), Metallogeny of Basic and Ultrabasic Rocks. The Institution of Mining and Metallurgy, London, U.K, pp. 415–425.

Marchesi, C., González-Jiménez, J.M., Gervilla, F., Garrido, C.J., Griffin, W.L., O'Reilly, S.Y., Proenza, J.A., Pearson, N.J., 2011. In situ Re–Os isotopic analysis of platinum-group minerals from the Mayarí–Cristal ophiolitic massif (Mayarí–Baracoa Ophiolitic Belt, eastern Cuba): implications for the origin of Os-isotope heterogeneities in podiform chromitites. Contrib. Mineral. Petrol. 161, 977–990.

Matveev, S., Ballhaus, C., 2002. Role of water in the origin of podiform chromitite deposits. Earth Planet. Sci. Lett. 203, 235–243.

Mendoza, O.T., 2000. Pre-accretion metamorphism of the Teloloapan Terrane (southern Mexico): example of burial metamorphism in an island-arc setting. J. S. Am. Earth Sci. 13, 337–354.

Mendoza, O.T., Suastegui, M.G., 2000. Geochemistry and isotopic com- position of the Guerrero Terrane (western Mexico): implication for the tectono-magmatic evolution of southwestern North America during the Late Mesozoic. J. S. Am. Earth Sci. 13, 297–324.

Mungall, J.E., 2002. Kinetic controls on the partitioning of trace elements between silicate and sulfide liquids. J. Petrol. 43, 749–768.

Mungall, J.E., 2005. Magmatic geochemistry of the platinum-group elements. In: Mungall, J.E. (Ed.), Exploration from platinum-group elements deposits. Short course series. Mineral. Assoc. Canada 35, pp. 1–34.

Mungall, J.E., Naldrett, A., 2008. Ore deposits of the platinum-group elements. Elements 4, 253–258.

Mungall, J.E., Brenan, J.M., 2014. Partitioning of platinum-group elements and Au between sulfide liquid and basalt and the origins of mantle-crust fractionation of the chalcophile elements. Geochim. Cosmochim. Acta 125, 265–289.

Murashko, V.I., Lavandero, R.M., 1989. Chromite in hyperbasite belt of Cuba. Int. Geol. Rev. 31, 90–99.

Naldrett, A.J., 2004. Magmatic Sulfide Deposits: Geology, Geochemistry and Exploration. Springer (728 pp).

Navrotsky, A., Mazeina, L., Majzlan, J., 2008. Size-driven structural and thermodynamic complexity in iron oxides. Science 319, 1635–1638.

O'Driscoll, B., González-Jiménez, J.M., 2016. Petrogenesis of the platinum-group minerals. Rev. Mineral. Geochem. 81, 489–578.

O'Neill, H.S.C., Dingwell, D.B., Borisov, A., Spettle, B., Palme, H., 1995. Experimental petrochemistry of some high side-rophile elements at high temperatures and some implications for core formation and the mantle's early history. Chem. Geol. 120, 255–273.

Ortiz-Hernández, L.E., Escamilla-Casas, J.C., Flores-Castro, K., Ramírez-Cardona, M., Acevedo-Sandoval, O., 2006. Características geológicas y potencial metalogenético de los principales complejos ultramáficos-máficos de México. Bol. Soc. Geol. Mex. 57, 161–181.

Ovtcharova, M., 2004. Petrology, geochronology and isotope studies on metagranitoids from the eastern part of the Madan–Davidkovo Dome (Ph.D. Thesis) University of Sofia, Sofia (235 pp).

Palenik, C.S., Utsunomiya, S., Reich, M., Kesler, S.E., Ewing, R.C., 2004. "Invisible" gold revealed: direct imaging of gold nanoparticles in a Carlin-type deposit. Am. Mineral. 89, 1359–1366.

Patten, C., Barnes, S.-J., Mathez, E.A., Jenner, F.E., 2013. Partition coefficients of chalcophile elements between sulfide and silicate melts and the early crystallization history of sulfide liquid: LA-ICP-MS analysis of MORB sulfide droplets. Chem. Geol. 358, 170–188.

Payakov, I., Zhelyaskova-Panayotova, M., Ivehinova, L., 1961. Structural–textural peculiarities and mineral composition of chromite ore from from Dobrimirtzi deposit. Annuarie de la Université de Sofia 56, 219–229.

Peach, C.L., Mathez, E.A., Keays, R.R., 1990. Sulfide melt-silicate melt distribution coefficients fro noble metals and other chalcophile elements as deduced from MORB: implications for partial melting. Geochim. Cosmochim. Acta 54, 3379–3389.

Peregoedova, A., Ohnenstetter, M., 2002. Collectors of Pt, Pd, and Rh in S-poor Fe-Ni-Cu sulfide system at 760 °C: experimental data and application to ore deposits. Can. Mineral. 40, 527–561.

Peregoedova, A., Barnes, S.-J., Baker, D.R., 2004. The formation of Pt–Ir alloys and Cu–Pd-rich sulfide melts by partial desulfurization of Fe–Ni–Cu sulfides: results of experiments and implications for natural systems. Chem. Geol. 208, 247–264.

Piña, R., Gervilla, F., Barnes, S.-J., Ortega, L., Lunar, R., 2015. Liquid immiscibility between arsenide and sulfide melts: evidence from a LA-ICP-MS study in magmatic deposits at Serranía de Ronda (Spain). Mineral. Deposita 50 (3), 265–279.

Prichard, H.M., Barnes, S.-J., Maier, W.D., Fisher, P.C., 2004. Variations in the nature of the platinum-group minerals in a cross section through the Merensky Reef at Impala platinum: implications for the mode of formation of the reef. Can. Mineral. 42, 423–437.

Prichard, H.M., Knight, R.D., Fisher, P.C., McDonald, I., Zhou, M.-F., Wang, C.Y., 2013. Distribution of platinum-group elements in magmatic and altered ores in the Jinchuan intrusion, China: an example of selenium remobilization by post magmatic fluids. Mineral. Deposita 48, 767–786.

Proenza, J.A., Gervilla, F., Melgarejo, J.C., Bodinier, J.L., 1999. Al- and Cr- rich chromitites from the Mayarí-Baracoa Ophiolitic Belt (eastern Cuba): consequence of interaction between volatile- rich melts and peridotite in suprasubduction mantle. Econ. Geol. 94, 547–566.

Proenza, J.A., Alfonso, P., Melgarejo, J.C., Gervilla, F., Tritlla, J., Fallick, A.E., 2003. D, O, C isotopes in podiform chromitites as fluid tracers for hydrothermal alteration processes of the Mayarí-Barcoa Ophiolitic Belt, eastern Cuba. J. Geochem. Explor. 78-79, 117–122.

Pruseth, K., Palme, H., 2004. The solubility of Pt in liquid Fe-sulfides. Chem. Geol. 208, 233–245.

Reich, M., Kesler, S.E., Utsunomiya, S., Palenik, C.S., Chryssoulis, S.L., Ewing, R.C., 2005. Solubility of gold in arsenian pyrite. Geochim. Cosmochim. Acta 69, 2781–2796.

Reich, M., Utsunomiya, S., Kesler, S.E., Wang, L.M., Ewing, R.C., Becker, U., 2006. Thermal behavior of metal nanoparticles in geologic materials. Geology 34, 1033–1036.

Reich, M., Chryssoulis, S.L., Deditius, A., Palacios, C., Zúñiga, A., Weldt, M., Alvear, M., 2010. "Invisible" silver and gold in supergene digenite (CuS). Geochim. Cosmochim. Acta 74, 6157–6173.

Reich, M., Hough, R., Deditius, A., Utsunomiya, S., Ciobanu, C., Cook, N.J., 2011. Nanogeoscience in ore systems research: principles, methods and applications. Ore Geol. Rev. 42, 1–5.

Reich, M., Vasconcelos, P., 2015. Geological and economic significance of supergene upgrading of metals. Elements 11, 305–310.

Reith, F., Fairbrother, L., Nolze, G., Wilhelmi, O., Clode, P., Gregg, A., Parsons, J.E., Wakelin, S.A., Pring, A., Hough, R., Southam, G., Brugger, J., 2010. Nanoparticle factories; biofilms hold the key to gold dispersion and nugget formation. Geology 38, 843–846.

Reith, R.F., Stewart, L., Wakelin, A., 2012. Supergene gold transformations: secondary and nano-particulate gold from southern New Zealand. Chem. Geol. 320-321, 32–45.

Reith, F., Zammit, C.M., Shar, S.S., Etschmann, B., Bottrill, R., Southam, G., Ta, C., Kilburn, M., Oberthür, T., Ball, A.S., Brugger, J., 2016. Biological role in the transformation of platinum-group mineral grains. Nat. Geosci. 9, 294–298.

Righter, K., Campbell, A.J., Humayun, M., Hervig, R.L., 2004. Partitioning of Ru, Rh, Pd, Re, Ir, and Au between Cr-bearing spinel, olivine, pyroxene and silicate melts. Geochim. Cosmochim. Acta 68, 867–880.

Rose, D., Viljoen, F., Knoper, M., Rajesh, H., 2011. Detailed assessment of platinum-group minerals associated with chromitite stringers in the Merensky Reef of the eastern Bushveld Complex, South Africa. Can. Mineral. 49, 1385–1396.

Roy-Barman, M., Wasserbur, G.J., Papanastasiou, D.A., Chaussidon, M., 1998. Osmium isotopic compositions and Re-Os concentrations in sulfide globules from basaltic glasses. Earth Planet. Sci. Lett. 154, 331–347.

Salgado-Terán, V., Serrano-Villar, J.F., 1983. Estudio geológico del yacimiento de níquel y cromo en rocas ultrabásicas, muni- cipios de Petatlán y Tecpan, estado de Guerrero. Unpublished BSc dissertation, Facultad de Ingeniería, Universidad Nacional Autónoma de México, Distrito Federal, Mexico, 65 p.

Saunders, J.A., 1990. Colloidal transport of gold and silica in epithermal precious-metal systems: evidence from the Sleeper deposit, Nevada. Geology 18, 757–760.

Scoates, J.S., Fiedman, R.M., 2008. Precise age of the platiniferous Merensky Reef, Bushveld Complex, South Africa, by the U-Pb zircon chemical abrasion ID-TIMS technique. Econ. Geol. 103, 465–471.

Snow, J.E., Schmidt, G., 1998. Constraints on Earth accretion deduced from noble metals in the oceanic mantle. Nature 391, 166–169.

Tarkian, M., Naidenova, E., Zhelyaskova-Panayotova, M., 1991. Platinum-group minerals in chromitites from the Eastem Rhodope Ultramafic Complex. Bulgaria. Mineral. Petrol. 44, 73–87.

Tredoux, M., Lindsay, N.M., Davies, G., McDonald, I., 1995. The fractionation of platinum-group elements in magmatic systems with the suggestion of a novel causal mechanism. S. Afr. J. Geol. 98, 157–167.

Vermaak, C.F., 1995. The Platinum-Group Metals – A Global Perspective. Mintek, Randburg, p. 247.

Wainwright, A.N., Luguet, A., Schreiber, A., Fonseca, R.O.C., Nowell, G.M., Lorand, J.-P., Wirth, R., .P.E., J., 2016. Nanoscale variations in 187Os isotopic compositions and HSE systematics in a Bultfontein peridotite. Earth Planet. Sci. Lett. (Submitted for publication).

Wirth, R., 2004. Focused Ion Beam (FIB): a novel technology for advanced application of micro- and nanoanalysis in geosciences and applied mineralogy. Eur. J. Mineral. 16, 863–876.

Wirth, R., 2009. Focused Ion Beam (FIB) combined with SEM and TEM: advanced analytical tools for studies of chemical composition, microstructure and crystal structure in geomaterials on a nanometre scale. Chem. Geol. 261, 217–229.

Wirth, R., Reid, D., Schreiber, A., 2013. Nanometer-sized platinum-group minerals (PGM) in base metal sulfides: new evidence for an orthomagmatic origin of the Merensky reef PGE ore deposit. Bushveld Complex. South Africa. Can. Mineral. 51, 143–155.

Wood, S.A., 2002. The aqueous geochemistry of the platinum-group elements with applications to ore deposits. In: L.J. (Ed.), The Geology, Geochemistry, Mineralogy and Mineral Beneficiation of Platinum-Group Elements. Canadian Institute of Minning, Metallurgy and Petroleum, Canada, pp. 211–249.

Zhmodik, S.M., Kalinin, Y.A., Roslyakov, N.A., Mironov, A.G., Mikhlin, Y.L., Belyanin, D.K., Nemirovskaya, N.A., Spiridonov, A.M., Nesternko, G.V., Airiyants, E.V., Moroz, T.N., Bul'bak, T.A., 2012. Nanoparticles of Noble metals in the supergene zone. Geol. Ore Deposits 54 (2), 141–154.

Zhelyaskova-Panayotova, M., Zinzov, Z., Pashov, 2000. Hydrothermal gold mineralization in ultrabasites near Dobromirtsi village, Kurdjali region. Annuaire de l'Université de Sofia 93 (1), 173–186.